Linkage between Substrate Recognition and Catalysis during Cleavage of Sarcin/Ricin Loop RNA by Restrictocin†

Alexei V. Korennykh,‡,§,|| Matthew J. Plantinga,⊥ Carl C. Correll,*⊥,@ and Joseph A. Piccirilli*,‡,§,⊥

Department of Chemistry, Department of Biochemistry and Molecular Biology, and Howard Hughes Medical Institute, The University of Chicago, Chicago, Illinois 60637

Received May 15, 2007; Revised Manuscript Received August 16, 2007

ABSTRACT: Restrictocin is a site-specific endoribonuclease that inactivates ribosomes by cleaving the sarcin/ricin loop (SRL) of 23S−28S rRNA. Here we present a kinetic and thermodynamic analysis of the SRL cleavage reaction based on monitoring the cleavage of RNA oligonucleotides (2−27-mers). Restrictocin binds to a 27-mer SRL model substrate (designated wild-type SRL) via electrostatic interactions to form a nonspecific ground state complex E:S. At pH 6.7, physical steps govern the reaction rate: the wild-type substrate reacts at a partially diffusion-limited rate, and a faster-reacting SRL, containing a 3′-sulfur atom at the scissile phosphate, reacts at a fully diffusion-limited rate ($k_2/K_{1/2} = 1.1 \times 10^9$ M^{-1} s^{-1}). At pH 7.4, the chemical step apparently limits the SRL cleavage rate. After the nonspecific binding step, restrictocin recognizes the SRL structure, which imparts 4.3 kcal/mol transition state stabilization relative to a single-stranded RNA. The two conserved SRL modules, bulged-G motif and GAGA tetraloop, contribute at least 2.4 and 1.9 kcal/mol, respectively, to the recognition. These findings suggest a model of SRL recognition in which restrictocin contacts the GAGA tetraloop and the bulged guanosine of the bulged-G motif to progress from the nonspecific ground state complex (E:S) to the higher-energy-specific complex (E·S) en route to the chemical transition state. Comparison of restrictocin with other ribonucleases revealed that restrictocin exhibits a 10^3−10^6-fold smaller ribonuclease activity against single-stranded RNA than do the restrictocin homologues, non-structure-specific ribonucleases T1 and U2. Together, these findings show how structural features of the SRL substrate facilitate catalysis and provide a mechanism for distinguishing between cognate and noncognate RNA.

Ribonucleases carry out essential processes in living cells, including RNA editing (*1*−*3*), signaling (*4*−*8*), and host protection (*9*, *10*). The enzymes exhibit a broad range of substrate specificities, with cleavage preferences for either specific nucleotides (*11*, *12*), specific sequences (*13*), or RNA structures (*4*, *6*, *14*, *15*). Structure-specific ribonucleases present attractive model systems for defining protein−RNA interactions quantitatively because they produce a conveniently detected signal (cleavage rate) and provide sensitive probes of protein−RNA recognition. The principles of protein−RNA recognition derived from this class of enzymes may have broad implications for a myriad of RNA-processing enzymes, which comprise 3−11% of bacterial and eukaryotic genomes (*16*).

Perhaps the best-studied structure-specific ribonucleases, and the focus of our work, are the endoribonucleases that cleave the sarcin/ricin loop of 23S−28S rRNA. These so-called ribotoxins, which include restrictocin, α-sarcin, and other related fungal ribonucleases, cleave the SRL[1] within the GAGA tetraloop (*14*) (Figure 1). The cleavage event inactivates ribosomes (*17*) and leads to cell death (*18*−*20*). The remarkable specificity of ribotoxins for cleavage of a single phosphodiester bond in rRNA has attracted much attention. The related ribonucleases T1 and U2, which share with ribotoxins sequence and structural homology, including active site composition (*21*), exhibit much broader specificity, cleaving single-stranded RNA on the 3′ side of guanosine and purine residues, respectively. Currently, we have only a limited understanding of the structural, energetic, and evolutionary bases of these differences in specificity.

Key insights into substrate recognition by ribotoxins have come from the work of Wool and colleagues (reviewed in ref *14*). They showed that α-sarcin retains cleavage specificity with an ∼30-mer RNA having the SRL sequence, indicating that ribotoxins recognize the SRL RNA in the absence of intact ribosomes. Biochemical analysis using the SRL oligonucleotides identified a critical nucleotide for α-sarcin-catalyzed cleavage, the conserved bulged guanosine located six nucleotides upstream from the cleavage site

† This work was supported by grants to A.V.K. from the Burroughs Wellcome Fund (1001774), to C.C.C. from the National Institutes of Health (GM59782), and to J.A.P. from the Howard Hughes Medical Institute.

* To whom correspondence should be addressed. J.A.P.: telephone, (773) 702-9312; fax, (773) 702-0271; e-mail, jpicciri@uchicago.edu. C.C.C.: telephone, (847) 578-8611; fax, (847) 578-3240; e-mail, carl.correll@rosalindfranklin.edu.

‡ Department of Chemistry.

§ Howard Hughes Medical Institute.

|| Present address: Department of Biochemistry and Biophysics, University of California San Francisco, San Francisco, CA 94158.

⊥ Department of Biochemistry and Molecular Biology.

@ Present address: Department of Biochemistry and Molecular Biology, Rosalind Franklin University of Medicine and Science, North Chicago, IL 60064.

[1] Abbreviations: SRL, sarcin/ricin loop RNA derived from rat 28S rRNA; E:S, nonspecific electrostatic complex; E·S, specific complex.

10.1021/bi700931y CCC: $37.00
Published on Web 10/12/2007

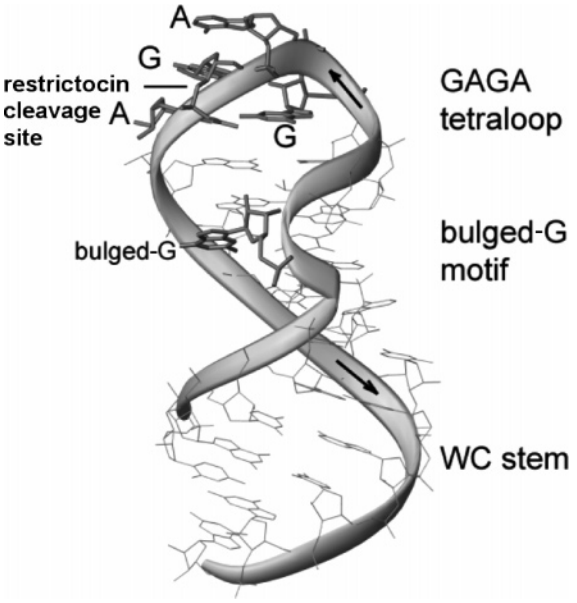

FIGURE 1: Tertiary structure of the sarcin/ricin loop RNA (SRL) derived from rat 28S rRNA. SRL oligonucleotides (~30-mers) fold independently, forming the same tertiary structure as in the ribosome. The SRL contains two universally conserved modules, the GAGA tetraloop and the bulged-G motif. Ribotoxins cleave the SRL site-specifically within the GAGA tetraloop (G4325 in rat 28S rRNA), as marked on the structure. The bulged-G, located six nucleotides upstream from the cleavage site, contributes to the specific cleavage of SRL by α-sarcin.

(G4325 in rat 28S rRNA). On the basis of these results and kinetic studies of insertion mutations, Wool et al. suggested that the ribotoxin binds to the bulged-G (designated the identity element) and then locates the cleavage site a fixed distance away (11 Å) (*22*).

Subsequent crystallographic analysis of restrictocin bound to SRL analogues has provided some support for this "molecular ruler" model. In one structure, the last A of the SRL's GAGA tetraloop docks into the active site, poised to undergo cleavage at the +1 register, but the ribotoxin makes limited contact with the bulged-G and no sequence-specific contacts to the bulged-G itself. By contrast, in a second structure, restrictocin makes numerous contacts with this motif, including sequence-specific hydrogen bonds to the solvent-exposed major groove face of the bulged-G, but only solvent molecules occupy the active site (*21*). Neither structure shows restrictocin making interactions simultaneously with the bulged-G and GAGA tetraloop. As a step toward elucidating how the tetraloop and bulged-G motif contribute to catalysis, we have characterized the kinetic pathway for the ribotoxin-mediated SRL cleavage reaction, with the aim of defining the structural and energetic principles underlying the specificity of the ribotoxin. We have chosen the ribotoxin restrictocin for this study due to the availability of structural data for restrictocin (*23*) and restrictocin complexes with SRL analogues (*21*).

MATERIALS AND METHODS

Ribotoxins. Restrictocin and α-sarcin were a gift from I. G. Wool. Restrictocin was also produced in our laboratory as described previously (*24*). Briefly, MQ cells were transformed with plasmid pREST and grown at 37 °C in four 1 L flasks in TB medium containing 100 mg/L ampicillin. When $A^{600} \sim 0.4$, cells were induced with 0.1 mM IPTG. The culture was incubated for an additional 4 h at 37 °C. Cells were harvested by centrifugation, suspended on ice in 30 mL of buffer containing 15 mM Tris-HCl (pH 7.4), 50 mM $MgCl_2$, and 20% (w/v) sucrose, and precipitated by centrifugation. The cell pellet was resuspended in ice-cold buffer containing 15 mM Tris-HCl (pH 7.4) and 50 mM $MgCl_2$. Supernatants from both steps contained protein and were combined and adjusted to pH 5.5 with 50 mM MES buffer. Protein was purified using cation-exchange chromatography and frozen in aliquots of 15 mM Tris-HCl buffer (pH 7.4). Active site titration confirmed that ~100% of the restrictocin sample used in this study was catalytically active.

RNA Substrates. RNA oligonucleotides were purchased from Dharmacon, Inc., synthesized in-house via phosphoramidite chemistry, or transcribed with T7 RNA polymerase in vitro. Prior to use, all RNA oligonucleotides were purified by 20% denaturing PAGE containing 8 M urea (or by 20% nondenaturing PAGE for SRL and SRL derivatives; see below). Gel slices containing RNA samples were eluted overnight in TE buffer [10 mM Tris-HCl (pH 7.4) and 1 mM K-EDTA] at 4 °C and desalted on C-18 SepPak cartridges. The eluates were lyophilized by SpeedVac and stored in water at −20 °C. Radioactive labeling of RNA termini with ^{32}P was accomplished using [γ-^{32}P]ATP and T4 polynucleotide kinase (NEB) for the 5′-terminus or [α-^{32}P]cordecypin and polyA polymerase (Ambion) for the 3′-terminus. Body labeled with [^{32}P]RNA was obtained by in vitro transcription with T7 RNA polymerase (NEB) in the presence of [α-^{32}P]UTP. Radioactive nucleotides were purchased from Perkin-Elmer.

SRL Oligonucleotide Contains a Restrictocin-Resistant Species. SRL RNA (5′-CCUGCUCAGUACGAGAGGAACCGCAGG) was purified by 20% denaturing polyacrylamide gel electrophoresis (DPAGE), which allows single-base resolution (*24*). SRL prepared in this way appeared homogeneous on DPAGE but exhibited biphasic kinetics during cleavage assays with restrictocin (Figure 2). Only 50−70% of the SRL gave the expected product, whereas the remaining 30−50% of the RNA resisted cleavage for more than 10 half-lives of the fast-cleaved fraction. This fraction of nonreactive material seemed unusually large compared to results with other RNA cleavage systems used in our laboratory. To test whether the fraction of unreactive SRL depends on the method used to synthesize it, we obtained SRL prepared by orthoester-based solid-phase synthesis (Dharmacon Inc.), by silyl-based solid-phase synthesis in our laboratory, and by in vitro transcription. All SRL preparations contained a restrictocin-resistant species (30−50%), suggesting that the SRL oligonucleotide has an inherent tendency to adopt a conformation (or form a chemically distinct species) that resists restrictocin cleavage.

We separated the "native" and "resistant" SRL forms using nondenaturing 20% PAGE (NPAGE). During NPAGE, two distinct bands formed from the SRL sample (Figure 2). These two bands comigrated during DPAGE. The fast-migrating band (S) reacted with restrictocin quantitatively, whereas the slow-migrating band (S*) resisted restrictocin cleavage. To delineate whether S and S* represent two equilibrium conformations of the SRL, we attempted to interconvert them by heating. Neither species produced the initial S/S* ratio

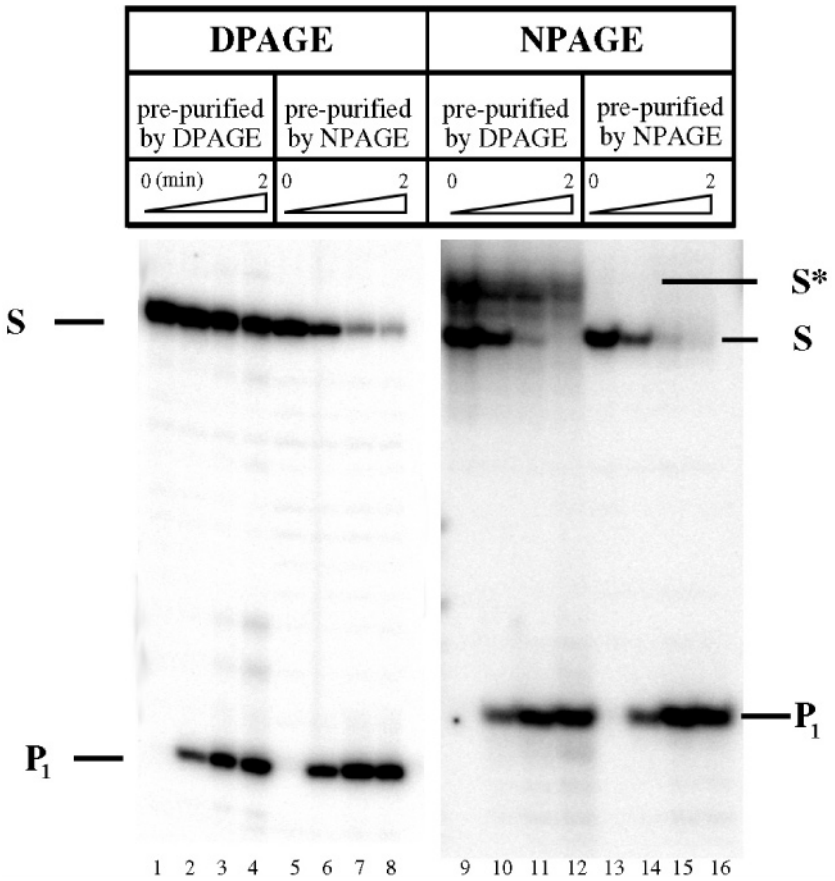

FIGURE 2: Structural and kinetic heterogeneity within SRL RNA (detected by nondenaturing gel electrophoresis). Time courses for SRL cleavage were analyzed by DPAGE and NPAGE. Reaction mixtures contained SRL purified by DPAGE only (SRL_D, lanes 1−4 and 9−12) or by NPAGE (SRL_N, lanes 5−8 and 13−16). NPAGE resolves SRL_D into two bands, only one of which reacts rapidly in the presence of restrictocin (lanes 9−12). SRL_D and SRL_N migrate as single bands during DPAGE (lanes 1−4 and 5−8, respectively). We purified the SRL studied here by NPAGE and isolated the species corresponding to the faster-migrating band in lane 9.

following three cycles of heating to 90 °C and cooling on ice. This lack of interconversion between the two species upon heating is puzzling, as the SRL contains only six Watson−Crick base pairs. At present, we do not know the difference between the two SRL populations. To separate the nonreactive fraction from the reactive fraction, we purified all SRL substrates used herein via NPAGE. The absence of rapid equilibration between S and S* suggests that we may also conduct kinetic measurements without this purification step as long as the data are corrected for the fraction of unreactive material.

RNA Cleavage Assay. Cleavage reactions, kinetic measurements, and quantitation were performed as described previously (*24*). In short, reaction buffer [10 mM Tris-HCl (pH 7.4), 0.05% (v/v) Triton X-100, and 0−300 mM KCl] containing 0.1 nM to 10 μM restrictocin was incubated at 37 °C for ~5 min. [^{32}P]RNA (for single-turnover reactions) or a mixture of radiolabeled and unlabeled RNA or inhibitor (for multiple-turnover reactions and inhibition studies, respectively) was then added to a final volume of 15 μL. Aliquots (1.5 μL) were withdrawn during a time course and placed in a stop solution containing 10 M urea, 0.2% SDS, and loading dyes. Samples were analyzed by 20% 29:1 PAGE (National Diagnostics) and quantified using a PhosphorImager (Molecular Dynamics). The data were analyzed using regression procedures in SigmaPlot 6.0.

Under low-salt conditions and at nanomolar restrictocin concentrations, restrictocin cleaved the SRL with irreproducible rates. We attributed this to nonspecific restrictocin adsorption and inactivation on the walls of the reaction tube. To improve the cleavage kinetics, we introduced the commonly used antisticking additives bovine serum albumin (BSA) and Triton X-100. Addition of BSA did not improve the assay reproducibility, but 0.05% Triton X-100 resulted in reproducible kinetics (Figure S1). Accordingly, we included 0.05% Triton X-100 in all reaction mixtures and restrictocin storage buffers that were used.

In further experiments, we encountered a different source of experimental uncertainty. Restrictocin cleaved ^{32}P-labeled SRL from different preparations with noticeably different rates. Dilution of the [^{32}P]SRL stocks with water improved the cleavage rates and lessened the variation (Figure S2). We suspect that the [^{32}P]SRL copurifies with inhibitory contaminants from the polyacrylamide gel used to purify the RNA. Upon drying the eluted SRL, we observed white residue on the bottom of the Eppendorf tubes, which could not be separated from the RNA sample with a SepPak C-18 column, phenol extraction, or ethanol precipitation of the RNA. We hypothesize that the samples may contain poly- and oligo-acrylamide that often cannot be separated from nucleic acids (*25*). Apparently, these moieties strongly inhibit restrictocin at low salt concentrations. Consistent with this hypothesis, blank slices of a PAGE gel that were processed in a manner analogous to that for the slices containing RNA samples yielded white material that, when dissolved, strongly inhibited the SRL cleavage reaction (Figure S2C). Strong

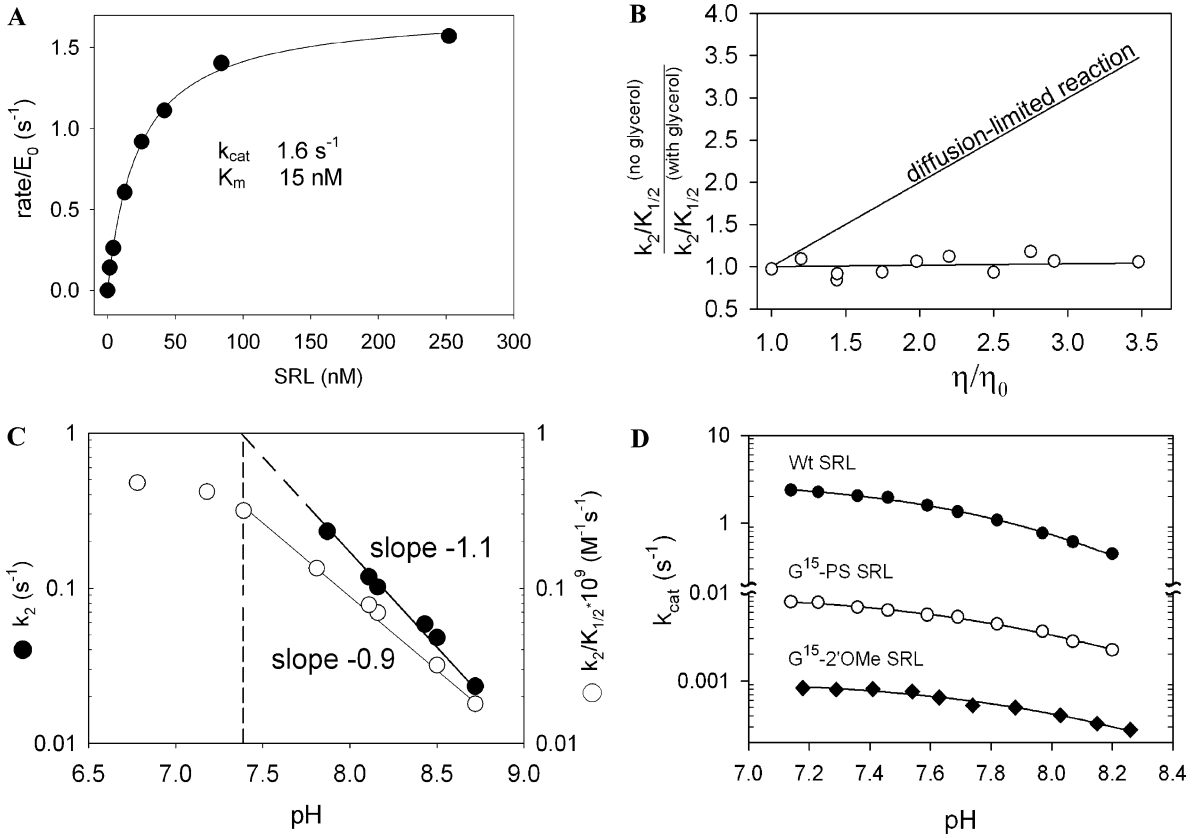

FIGURE 3: Rate-limiting step of restrictocin-catalyzed SRL cleavage. (A) Dependence of the reaction rate on SRL concentration. Reactions were multiple-turnover and conducted at 37 °C, and they contained 1 nM restrictocin, [^{32}P]SRL as indicated, 10 mM Tris-HCl (pH 7.4), and 0.05% Triton X-100. A fit of the data to a hyperbolic binding curve gives the following kinetic parameters: $k_{cat} = 1.6 \pm 0.4$ s^{-1} and $K_m = 15 \pm 4$ nM. (B) Dependence of the second-order rate constant ($k_2/K_{1/2}$) for restrictocin-catalyzed SRL cleavage on buffer viscosity (○). Reactions were single-turnover under the conditions described for panel A, but the mixtures contained <1 nM [^{32}P]SRL and 0−40% glycerol. The solid line represents the expected viscosity dependence for a diffusion-limited reaction. Relative buffer viscosity (η/η_0) at 37 °C was determined by capillary viscosimetry (Materials and Methods). (C) Estimation of the single-turnover rate constant k_2 for the SRL cleavage reaction at pH 7.4 by extrapolation of the pH−rate profile (●). Reactions were conducted at 37 °C, and mixtures contained 1 μM restrictocin and <1 nM radiolabeled [^{32}P]SRL. (D) Restrictocin cleaves differentially reactive RNA substrates with similar pH−rate profiles: wild-type SRL (●), SRL containing a racemic phosphorothioate linkage at the scissile position (○), and SRL containing a 2′-OMe substitution at the scissile position, which reacts at nonspecific sites (◆). Reactions were conducted as described for panel A, but mixtures contained 100 nM SRL, 5 nM restrictocin, and <1 nM ^{32}P-labeled wild-type SRL (●), 100 nM restrictocin and <1 nM ^{32}P-labeled phosphorothioate-substituted SRL (○), or 100 nM restrictocin and <1 nM ^{32}P-labeled 2′-OMe-substituted SRL (◆). The data fit best using an equation describing two inhibitory deprotonation events in the E:S complex with acidity constants pK_{a1} and pK_{a2} (Materials and Methods). The titration profiles give a common pK_{a1} of 7.8 ± 0.1 and a pK_{a2} of 8.1 ± 0.2 for the wild-type SRL, a pK_{a2} of 8.8 ± 0.9 for the phosphorothioate-containing SRL, and a pK_{a2} of 8.9 ± 0.8 for the 2′-OMe-substituted SRL.

inhibition also occurred upon addition of linear polyacrylamide polymerized without cross-linker to the SRL cleavage reaction mixture (Figure S2D). To minimize the impact of these inhibitory contaminants on the reproducibility of the experiments, we consistently diluted all ^{32}P-labeled substrates in 1 mL of water per 20 pmol of radiolabeled SRL, unless stated otherwise. This protocol resulted in a <2-fold variation in cleavage rates among different SRL preparations.

Fitting the pH Dependence. The pH profiles for wild-type SRL cleavage did not fit inhibitory deprotonation of a single residue. Adequate fits were obtained using a model for inhibitory deprotonation of two restrictocin residues having pK_{a1} and pK_{a2}:

$$E + H^+ \overset{pK_{a1}}{\rightleftharpoons} EH^+ + H^+ \overset{pK_{a2}}{\rightleftharpoons} EH_2^{2+}$$

where E, EH^+, and EH_2^{2+} correspond to unprotonated and two different protonated restrictocin forms. All forms bind to the SRL with the same affinity, but only the EH_2^{2+} form has enzymatic activity. Equation 1 obtained from the above scheme was used to fit the data in Figure 3D:

$$k_{obs} = k_{obs}^{max}/(1 + 10^{pH-pK_{a1}} + 10^{2pH-pK_{a1}-pK_{a2}}) \quad (1)$$

where k_{obs} is the observed rate constant (s^{-1}), k_{obs}^{max} is the observed rate constant for the fully protonated enzyme (that exists below pH 7 in Figure 3D), and pK_{a1} and pK_{a2} are the apparent pK_a's of the two catalytic residues. Below pH 8, cleavage of the SRL and the nonspecific substrates exhibits sensitivity to a single deprotonation event with an apparent pK_a of ~7.8, consistent with the possibility that pH dependencies for the reactions of all three substrates reflect titration of the same residue (Figure 3D).

Viscosity Measurements. Viscosity of glycerol-containing buffers was determined by Ostwald's method from the rate of liquid flow through a capillary (*26*). Experiments were conducted at an ambient temperature of 37 °C using reaction buffers that contained 10 mM Tris-HCl (pH 7.4), 0.05% (v/

Scheme 1. Kinetic Framework for Restrictocin-Catalyzed Cleavage of Sarcin/Ricin Loop 27-mer (SRL) at 37 °C in 10 mM Tris-HCl (pH 7.4), 5 mM KCl, and 0.05% Triton X-100[a]

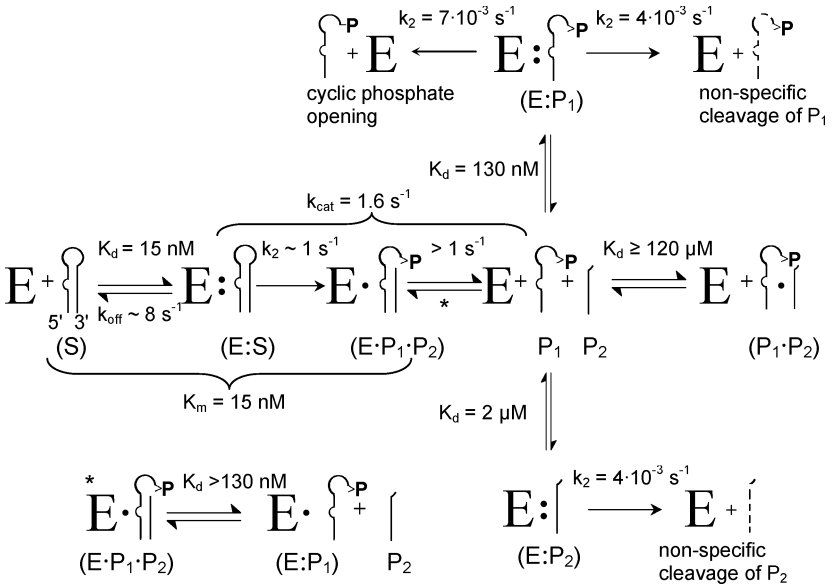

[a] Restrictocin binds SRL with an affinity of ~15 nM and cleaves the enzyme−substrate (E:S) complex with a k_2 of ~1 s^{-1}. The products of SRL cleavage bind weakly and do not inhibit the cleavage reaction; the 5′-product of SRL cleavage, P_1, contains a 2′,3′-cyclic phosphodiester. E refers to restrictocin. S refers to SRL. P_1 and P_2 refer to 5′- and 3′-products, respectively. K_d is the dissociation constant (molar). k_2 and k_{cat} are single- and multiple-turnover first-order rate constants, respectively (s^{-1}). k_{off} is the dissociation constant (s^{-1}). Nonspecific cleavage occurs in multiple sites predominantly after G and A residues as in Figure 4B.

v) Triton X-100, and 0−40% glycerol. The experimental uncertainty between measurements was less than 10%.

Experimental Errors. All experiments described here were repeated two or more times. The reported values for the kinetic parameters are averages derived from all available measurements. Uncertainties normally were within ±20% and did not exceed ±50%, unless noted otherwise. Experimental uncertainties are provided in the text where appropriate.

RESULTS

Overview. To provide a baseline framework for exploring the specificity determinants and catalytic mechanism of restrictocin, we conducted kinetic and thermodynamic measurements to define the minimal reaction scheme (Scheme 1) and reveal the nature of the rate-limiting step(s), determined the variation in these measurements with respect to salt concentration and pH, established the nature and origin of the products, and defined the enzyme's specificity and fidelity operationally. We then used this framework to explore effects of substrate modifications on cleavage and to compare restrictocin with related non-structure-specific ribonucleases.

Assay for Quantitative Analysis of the Restrictocin-Catalyzed SRL Cleavage Reaction. Previously, we showed that the affinity of SRL for restrictocin and the second-order rate constant for SRL cleavage under single-turnover conditions ($k_2/K_{1/2}$) depend strongly on the salt concentration in the reaction buffer, decreasing linearly in double-logarithmic coordinates as the salt concentration increases, with a slope n of -4.2 ± 0.3 (*24*). Here, we show that the slope of the salt dependence increases as the oligonucleotide length increases and reaches a plateau of $n = -4.2$ at 20 nucleotides (Figure S3). This salt dependence on binding arises from electrostatic interactions between the cationic residues of restrictocin and the phosphates of oligonucleotide substrates and reflects competition between salt ions and the enzyme for binding to the RNA substrate. Formation of the bound complex is adequately described by a nonlinear Poisson−Boltzmann model, which correctly predicts a slope n^{theor} of −4.2 for the formation of the restrictocin−SRL complex based on a crystal structure (PDB entry 1JBS) (A. V. Korennykh, M. J. Plantinga, C. C. Correll, and J. A. Piccirilli, unpublished). As expected (*27*), mutating basic residues outside the restrictocin−SRL interface (*21*) has no effect on the slope of the salt dependence (*24*), whereas mutating interface residues reduces the slope (M. J. Plantinga, A. V. Korennykh, J. A. Piccirilli, and C. C. Correll, unpublished results). In contrast to the effect on binding, the k_{cat} of 1.6 s^{-1} (multiple-turnover catalytic constant) showed no dependence on the salt concentration. At low KCl concentrations (<5 mM), electrostatic interactions strengthen such that restrictocin binds tighter to the SRL ($K_m = 15$ nM vs $K_m = 76$ μM at 50 mM KCl) and exhibits large values of single- and multiple-turnover kinetic parameters: $k_2/K_{1/2} = 10^8$ M^{-1} s^{-1} and $k_{cat}/K_m = 10^8$ M^{-1} s^{-1} (*24*). The single- and multiple-turnover kinetic parameters for the SRL cleavage reaction are similar, indicating rapid product release (see below). This agreement allows comparison of experiments conducted in either regime and simplifies interpretation of the results from kinetic measurements.

The strong salt sensitivity of restrictocin-catalyzed SRL cleavage is unexpected on the basis of previous work with the homologous ribotoxin, α-sarcin [sequence 86% identical with that of restrictocin (*14*)]. α-Sarcin was shown to cleave the SRL at a constant rate between 0 and 100 mM KCl (*28*). Over the same range of KCl concentrations, restrictocin exhibited a 10^6-fold decrease in the observed rate constant (*24*). To investigate the origin of this discrepancy, we examined the reaction conditions under which the α-sarcin

data were obtained. We noted that the previous study was conducted using 30 μM α-sarcin, which induces saturating (k_2) conditions below 130 mM KCl and makes changes in the binding affinity undetectable. When the α-sarcin concentration is reduced to ensure subsaturating ($k_2/K_{1/2}$) conditions, the reaction rate acquires a strong dependence on the KCl concentration ($n = -4.8$) (*24*). This salt dependence of $k_2/K_{1/2}$ reflects changes in $K_{1/2}$: the SRL reacts with $K_{1/2}$ values of 5 nM and 4 μM at 5 and 100 mM KCl, respectively. These findings for α-sarcin are consistent with those for restrictocin and demonstrate the importance of electrostatic interactions in the ground state E:S complex of both ribotoxins.

Developing a Quantitative Framework for the SRL Cleavage Reaction (Scheme 1). Under multiple-turnover conditions (1 nM restrictocin and 2−250 nM SRL, with 10 mM Tris-HCl at pH 7.4 and 37 °C), restrictocin cleaves the SRL with a k_{cat} of 1.6 ± 0.4 s^{-1} and a K_m of 15 ± 4 nM (Figure 3A), forming two products, designated herein as P_1 and P_2 (Scheme 1). In single-turnover reactions ($[E_0] \gg [S_0]$), the corresponding kinetic parameters, k_2 and $K_{1/2}$, have values similar to those of the corresponding multiple-turnover parameters, suggesting that product release happens faster than the chemical step. At pH 7.4, the $k_2/K_{1/2}$ exhibits no dependence on the solvent viscosity (Figure 3B), suggesting that the physical step of substrate binding does not limit the reaction rate and that the rate-limiting step occurs after the enzyme−substrate association and either prior to or during the chemical step. At pH 7.4, dissociation of the SRL from the E:S complex must occur faster than conversion of SRL to products such that $K_m = K_d$. Further supporting the assertion that $K_m = K_d$, noncleavable SRL analogues containing 2′-deoxyguanosine or 2′-methoxyguanosine at the specific cleavage site competitively inhibit SRL cleavage with K_i values equal to the K_m of SRL.

P_1 and P_2 Bind Weakly to Restrictocin and Undergo Slow Nonspecific Cleavage. The products of SRL cleavage, P_1 and P_2, undergo further cleavage by restrictocin predominantly at guanosine residues (Scheme 1). To investigate the interaction of the SRL cleavage products with restrictocin, we obtained radiolabeled forms of P_1 and P_2 via cleavage of [5′-^{32}P]SRL and [^{32}P]CoATP-3′-SRL, respectively. The radiolabeled products [5′-^{32}P]P_1 and [^{32}P]CoATP-3′-P_2 were purified by PAGE and used as substrates in independent assays with restrictocin. We determined the $K_{1/2}$ and k_2 values for reaction of P_1 and P_2 (Scheme 1) under single-turnover conditions (<1 nM [^{32}P]RNA, 1−5 μM restrictocin) by measuring the restrictocin concentration dependence of P_1 and P_2 cleavage. P_1 and P_2 react with a 10^3-fold slower k_2 than the SRL and bind to restrictocin 9- and 130-fold more weakly than the SRL, respectively.

The P_1·P_2 Duplex Dissociates following SRL Cleavage. We used RNase T1 protection to determine the stability of the P_1·P_2 duplex (Figure S4). RNase T1 cleaves RNA after guanosines in single-stranded regions. To determine the stability of the P_1·P_2 duplex, we used an inhibition assay in which P_2 competes with RNase T1 for binding to free P_1 (Figure S4). In reaction mixtures containing ^{32}P-labeled P_1 and 18 nM RNase T1, increasing concentrations of P_2 inhibited P_1 degradation with an apparent K_i of 120 μM [Figure S4C (●)]. Inhibition arises either from binding of P_2 to P_1 or from direct inhibition of RNase T1 by P_2 (pathways 1 and 2 in Figure S4B). Therefore, the apparent K_i provides a lower limit for the equilibrium dissociation constant of the P_1·P_2 duplex. The large value of K_i indicates that the P_1·P_2 duplex is not stable under the conditions of the restrictocin cleavage assay. We verified that the RNase T1 protection assay provides a suitable measure of the association between RNA strands by replacing P_2 with a 12-mer RNA (designated here as 12-CMP) with full complementarity to nucleotides 1−12 of P_1. 12-CMP inhibited cleavage of P_1 by RNase T1 with a K_i of 32 nM [Figure S4C (△)], which likely represents the K_d for dissociation of the P_1·12-CMP duplex.

Although P_2 and P_1 interact weakly with each other, positively charged restrictocin could neutralize the repulsive electrostatic interaction between RNA strands in the restrictocin·P_1·P_2 ternary complex. As restrictocin preferentially cleaves single-stranded RNA (Figure S5), cleavage of P_1 should be slower in the restrictocin·P_1·P_2 ternary complex than in the restrictocin·P_1 complex. However, adding P_2 (0−500 nM) to the reaction mixture containing <1 nM [^{32}P]P_1 and 1.6 μM restrictocin (12-fold the K_m for P_1) had no effect on cleavage of P_1, suggesting that the concentration of the restrictocin·P_1·P_2 ternary complex does not build up under these conditions. We infer that the restrictocin·P_1·P_2 ternary complex likely dissociates rapidly following SRL cleavage.

P_1 Contains a 2′,3′-Cyclic Phosphate. α-Sarcin cleaves ApA and GpA dinucleotides to form products that contain a 2′,3′-cyclic phosphate, which react further to give the corresponding 3′-terminal phosphate monoesters (*29*). To track the fate of the scissile phosphate in the SRL cleavage reaction, we constructed a SRL substrate containing a ^{32}P label at the cleavage site, designated here as SRL^P (Figure S6). Restrictocin-catalyzed cleavage of SRL^P generated P_1 bearing ^{32}P phosphate at its 3′-terminus. As expected, P_1 retained this label following treatment with alkaline phosphatase, consistent with the presence of a 2′,3′-cyclic phosphate diester (Figure S7). Incubation of this P_1 with higher restrictocin concentrations generated a product that rapidly releases the radioactivity (^{32}P) upon phosphatase treatment (Figure S7). This result suggests that restrictocin slowly opens the cyclic phosphate, resulting in a terminal phosphate monoester that becomes hydrolyzed upon phosphatase treatment. SDS−PAGE followed by silver staining did not detect contaminating proteins in the restrictocin sample, suggesting that the 2′,3′-cyclic phosphodiesterase activity arises from restrictocin. Further supporting this possibility, the $K_{1/2}$ of ∼300 nM for opening of the cyclic phosphate agrees reasonably well with the $K_{1/2}$ of ∼130 nM for cleavage of P_1 (Scheme 1). This agreement suggests that the same enzyme carries out both cleavage of the backbone of P_1 and opening of the 2′,3′-cyclic phosphate on its 3′-terminus.

Rate-Limiting Step of the SRL Cleavage Reaction. Under our standard reaction conditions (37 °C, 10 mM Tris-HCl, pH 7.4, and 0.05% Triton X-100, where $[E_0] \gg [S_0]$), restrictocin cleaves the SRL oligonucleotide with the second-order rate constant ($k_2/K_{1/2}$) of 10^8 M^{-1} s^{-1}. As stated above, this rate constant shows no dependence on buffer viscosity (Figure 3B), indicating that physical steps involved in enzyme−substrate association do not limit the reaction rate.

To determine whether dissociation of the products limits the rate of restrictocin-catalyzed SRL cleavage, we compared

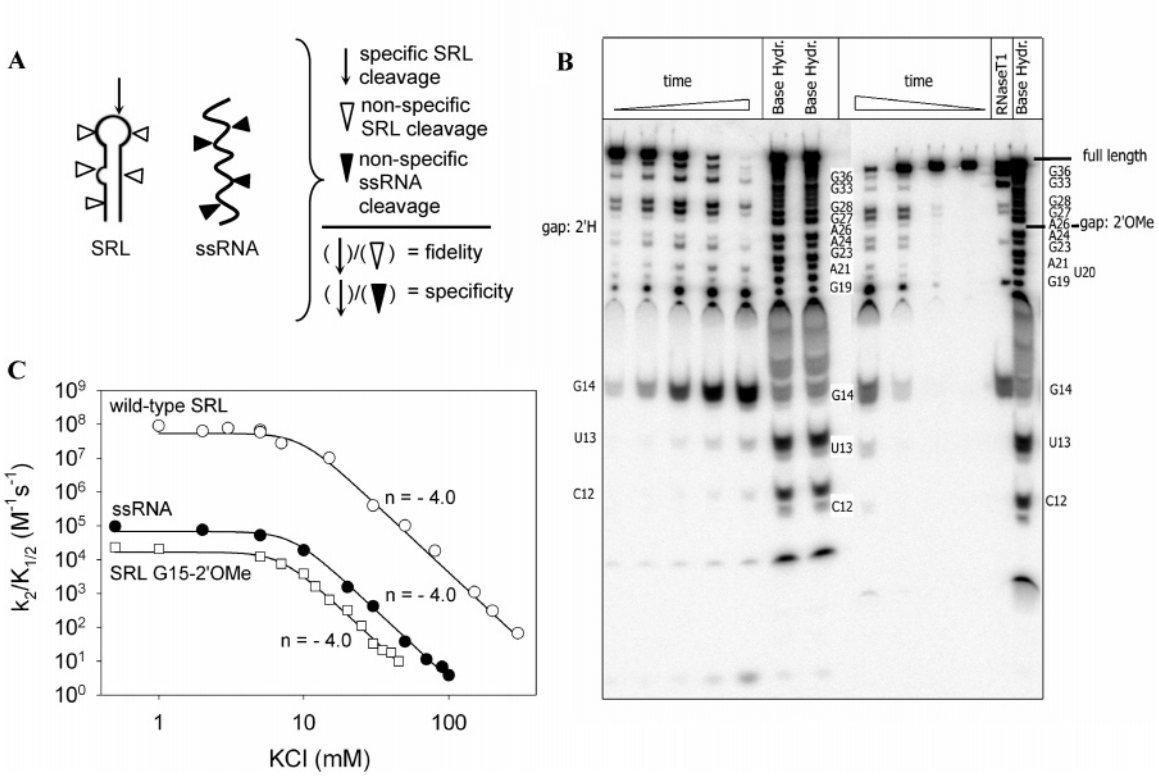

FIGURE 4: Quantitative assessment of fidelity and specificity for SRL cleavage by restrictocin. (A) Fidelity is defined as the ratio of second-order rate constants $k_2/K_{1/2}$ for specific SRL cleavage (cleavage site arrow) vs nonspecific SRL cleavage (white arrowheads). To assess the rate of nonspecific SRL cleavage, we used substrates containing 2′-deoxyguanosine or 2′-methoxyguanosine at the cleavage site, thereby blocking the pathway for specific cleavage. Specificity is defined as the ratio of second-order rate constants $k_2/K_{1/2}$ for specific SRL cleavage vs nonspecific cleavage of unstructured single-stranded RNA (black arrowheads). (B) Cleavage time courses for 2′-OMe- and 2′-H-substituted SRL oligonucleotides. Reactions were conducted at 37 °C, and mixtures contained 1 μM restrictocin, <1 nM RNA (5′-^{32}P-CCUGCUCAGUACGA**G**$_{2'x}$**A**GGAACCGCAGG, where x = 2′-OMe or 2′-H), 10 mM Tris-HCl (pH 7.4), 50 mM KCl, and 1 mM K-EDTA (Results). (C) Effect of KCl concentration on the second-order rate constant ($k_2/K_{1/2}$) for restrictocin-catalyzed cleavage of wild-type SRL (○), 2′-OMe-substituted SRL (□), and ssRNA [5′-^{32}P-UAGUAGUG**GA**GAGACAGCAGCCGACAC (●)]. Reactions were conducted at 37 °C, and mixtures contained 1 nM to 10 μM restrictocin, 10 mM Tris-HCl (pH 7.4), 0.05% Triton X-100, and KCl as indicated.

the catalytic constants k_2 and k_{cat} obtained under single-turnover ([E_0] ≫ [S_0]) and multiple-turnover ([S_0] ≫ [E_0]) conditions, respectively (Scheme 1). If product release limited the reaction rate under multiple-turnover conditions, then the multiple-turnover rate constant k_{cat} would be smaller than the single-turnover constant k_2. The rate constant k_2 could not be measured directly at pH 7.4 due to rapid SRL cleavage in the presence of excess restrictocin. Therefore, we estimated k_2 by extrapolation of the pH−rate profile, which gives a k_2 of 1.0 ± 0.2 s^{-1} at pH 7.4 (Figure 3C). The similar pH dependence of $k_2/K_{1/2}$ [Figure 3C (○)] suggests that linear extrapolation of k_2 to pH 7.4 is appropriate. The k_2 value (1 s^{-1}) does not exceed the k_{cat} (1.6 s^{-1}), strongly suggesting that product release occurs faster than substrate cleavage (Figure 3A,C and Scheme 1). The similarity of the single- and multiple-turnover catalytic constants together with the absence of viscosity dependence indicates that the rate-limiting step for SRL cleavage occurs during conversion of the ground state complex (E:S) to products.

To explore the rate-limiting step further, we determined the kinetic parameters for several substrates that react significantly slower than the SRL. We obtained the pH−rate profiles for restrictocin-catalyzed cleavage of the following substrates: (i) wild-type SRL, (ii) SRL containing a nonbridging phosphorothioate at the scissile position, (iii) SRL with the specific cleavage site blocked by a 2′-OMe substitution so that cleavage occurs at only nonspecific sites [2′-OMe SRL (Figure 4)], and (iv) a single-stranded 27-mer RNA lacking secondary structure (ssRNA). The phosphorothioate substitution decreases the rate of restrictocin-catalyzed SRL cleavage by more than 100-fold, whereas 2′-OMe SRL and ssRNA react 1000-fold slower (Figures 3, 4, and S8). These substrates react with analogous pH−rate profiles, consistent with the involvement of the same protonated group(s) on the enzyme in the rate-limiting step of their cleavage (Figures 3D and S8). The similar pH−rate profiles for the SRL and ssRNA suggest that the rate-limiting step does not involve structural rearrangements specific to the SRL fold.

To test whether the chemical step limits the rate of SRL cleavage, we prepared a SRL bearing a 3′-sulfur atom at the scissile phosphate (designated 3′S-SRL). In nonenzymatic reactions, a 3′-phosphorothioate reacts ∼2000-fold faster than normal phosphodiesters (*30*). If the chemical step limited the restrictocin-catalyzed cleavage, the 3′S-SRL might react faster than wild-type SRL, due to the inherently higher reactivity of the modified scissile linkage. In the presence of subsaturating restrictocin concentrations [1 nM restrictocin, <1 nM [^{32}P]3′S-SRL, 10 mM Tris-HCl (pH 7.4), and 0.05% Triton X-100], the 3′S-SRL reacted 5-fold faster than the wild-type SRL (Figure 5), consistent with the possibility that the chemical step limits the rate of wild-type SRL

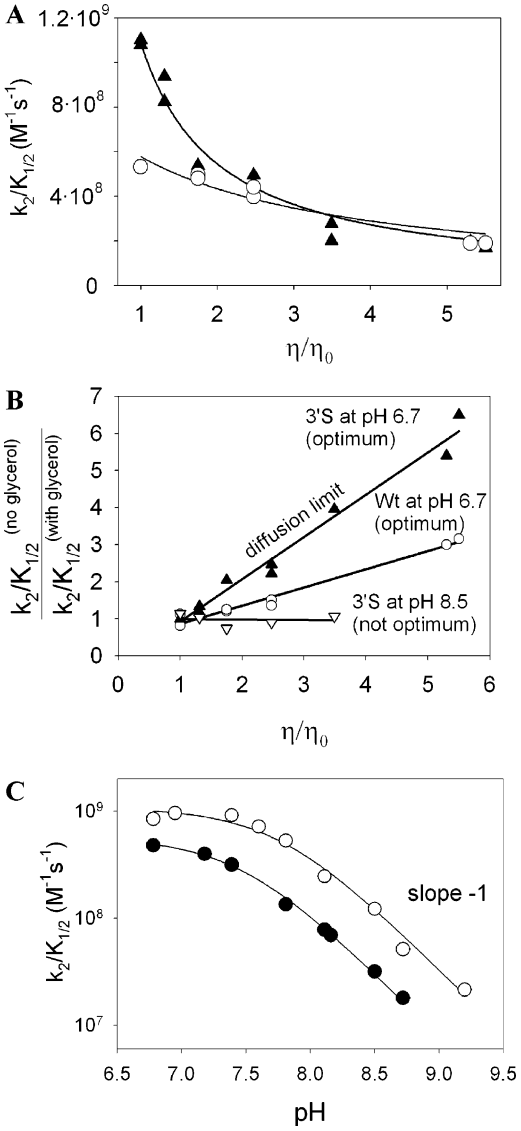

FIGURE 5: Diffusion limits restrictocin-catalyzed SRL cleavage at pH 6.7. (A) Viscosity dependencies for the rates of restrictocin-catalyzed cleavage of wild-type SRL (○) and 3′S-SRL (▲) at pH 6.7. Reaction mixtures contained 0.1 nM restrictocin, <0.1 nM radiolabeled [^{32}P]SRL, 10 mM BisTris-HCl (pH 6.7), 0.05% Triton X-100, and 0−40% glycerol. Relative buffer viscosity (η/η_0) was determined by capillary viscosimetry (Materials and Methods). (B) Normalized reciprocal plot of the data in panel A. (C) pH profiles for cleavage of wild-type SRL (●) and 3′S-SRL (○). Reactions were conducted as described for panel A.

cleavage. Nevertheless, the sulfur atom gives much weaker stimulation in the restrictocin-catalyzed reaction than in the nonenzymatic reaction. Perhaps the 3′S-SRL docks less favorably into the active site or gains less transition state stabilization due to steric perturbation by the 3′S atom, thereby offsetting the increased chemical reactivity of the 3′S-SRL. Alternatively, for 3′S-SRL, a different step might become rate-limiting, thereby masking the greater intrinsic increase in the chemical reactivity.

The latter possibility appears unlikely, considering the similar pH−rate profiles for cleavage of the 3′S-SRL and the unmodified SRL (Figure 5C). At pH >7.5, the 3′S-SRL reacts 5−6-fold faster than the unmodified SRL throughout the pH range, providing no evidence of different rate-limiting steps between wild-type SRL and 3′S-SRL. We therefore favor the hypothesis that the chemical step limits the cleavage rate for both substrates at pH 7.5. At pH <7.5, the reaction rates for 3′S-SRL and wild-type SRL begin to converge [between pH 6.7 and 7.5, 3′S-SRL reacts with little dependence on pH (Figure 5C)]. At pH 6.7, 3′S-SRL reacts only 2.0 ± 0.5-fold faster than wild-type SRL (Figure 5A). This change in relative reactivity vs pH may reflect a shift in the rate-limiting step.

Physical Limit for SRL Cleavage. Cleavage of the SRL by restrictocin at pH 7.4 occurs with a second-order rate constant ($k_2/K_{1/2}$) of 10^8 M^{-1} s^{-1} and exhibits no dependence on viscosity (Figure 3B). To examine whether this cleavage reaction encounters the diffusion limit at the optimal pH [pH 6.0−7.0 (*24*)], we carried out restrictocin-catalyzed SRL cleavage at pH 6.7. Under these conditions, the SRL reacts with a second-order rate constant ($k_2/K_{1/2}$) of 5×10^8 M^{-1} s^{-1} and acquires the viscosity dependence of a partially (*31*) diffusion-controlled rate (Figure 5A,B). For such reactions, dissociation of the ground state E:S complex to E + S and conversion of E:S to products happen with similar rates.

Under the same conditions (10 mM Tris-HCl, pH 6.7, and 0.05% Triton X-100) but not at suboptimal pH 8.5 [Figure 5B (▽)], 3′S-SRL reacts with a $k_2/K_{1/2}$ of 1.1×10^9 M^{-1} s^{-1} and exhibits the viscosity dependence of a fully diffusion-limited reaction [Figure 5A,B (▲)]. The $k_2/K_{1/2}$ value therefore gives the rate constant for restrictocin−SRL association (k_{on}), the physical limit for the rate of SRL cleavage. Under diffusion-limited conditions, the binary E:S complex reacts faster than it dissociates ($k_{off} \ll k_2$) so that k_2 provides an upper limit for k_{off}. At pH 6.7, the 3′S-SRL reacts too fast to measure k_2 directly, but we may estimate the value for this rate constant at pH 6.7 as follows. Extrapolation of the k_2 pH−rate profile for wild-type SRL to pH 7.4 gives a k_2 (SRL) of ∼1 s^{-1}. Under $k_2/K_{1/2}$ conditions at pH 6.7, wild-type SRL reacts 2-fold faster than at pH 7.4 [Figure 5C (○ vs ●)]. As $K_{1/2}$ exhibits little or no dependence on pH [the SRL reacts with similar pH−rate dependencies under k_2 and $k_2/K_{1/2}$ conditions (Figure 3C)], we conclude that at pH 6.7, k_2 for wild-type SRL is 2-fold faster than at pH 7.4 or ∼2 s^{-1}. The 3′S-SRL reacts no more than 6-fold faster than wild-type SRL (Figure 5). Accordingly, we estimate that the 3′S-SRL reacts at pH 6.7 with a k_2 of ≤12 s^{-1} (2 s^{-1} × 6). This k_2 estimate provides the upper limit for k_{off} of 12 s^{-1}.

We may estimate a lower limit for k_{off} from k_2 for the wild-type SRL at pH 7.4 (Figure 3C). At pH 7.4, wild-type SRL cleavage occurs slower than the diffusion limit with a k_2 of 1 s^{-1}, suggesting that the SRL dissociates from restrictocin with a k_{off} of >1 s^{-1}. Combining the upper (pH 6.7) and lower (pH 7.4) limits gives a k_{off} between 1 and 12 s^{-1} (assuming that k_{off}, like $K_{1/2}$, does not vary appreciably over this pH range). We may also estimate k_{off} using the k_{on} value of 1.1×10^9 M^{-1} s^{-1} and the equilibrium dissociation constant (K_d) for the SRL. We measured K_d in the range of 2−15 nM (8 nM on average) depending on the dilution of SRL [the variation arises from the inhibitory contaminant from PAGE, as described above (Figure S2)]. From these values, we estimate that $k_{off} = K_d k_{on} \sim 8$ s^{-1}, within the limit estimated above.

Specificity and Fidelity of the SRL Cleavage Reaction. To probe the free energy determinants of SRL recognition by restrictocin, we defined measures for the specificity and fidelity of the cleavage reaction. To assess the specificity,

we compared the cleavage rate for the SRL with the cleavage rate for single-stranded RNA (ssRNA) containing a GA sequence. Under $k_2/K_{1/2}$ conditions, restrictocin cleaves the SRL 10^3-fold faster than the ssRNA, providing an empirical measure of the specificity (4.3 kcal/mol). This quantitative measure agrees with the finding that ribotoxins target one phosphodiester bond out of several thousand in the ribosomal RNA (*32*). The ssRNA substrate binds to restrictocin with the same affinity as does the SRL but reacts from the binary complex 10^3-fold more slowly ($k_2^{ssRNA} = 0.001\ s^{-1}$, $k_2^{SRL} = 1\ s^{-1}$). Fidelity refers to the ability of restrictocin to discriminate between sites within the same substrate (Figure 4A). To assess the ability of restrictocin to cleave the SRL substrate at alternate sites, we blocked cleavage at the correct site (G4325 in the 28S rat rRNA sequence) by replacing G4325 with either 2′-methoxyguanosine or 2′-deoxyguanosine. These modified substrates bind to restrictocin with the same affinity as does the wild-type SRL but react 700-fold more slowly (Figure 4B,C). The nonspecific cleavage of these substrates occurs at approximately six sites, giving a normalized per-site fidelity of $700 \times 6 = 4200$ (5.1 kcal/mol).

The $k_2/K_{1/2}$ values for the reaction of ssRNA, SRL, and 2′-substituted SRL substrates vary with the same salt dependence (Figure 4C) and pH dependence (pH 7.2−8.2). Although the absolute values of $k_2/K_{1/2}$ decrease by $>10^6$-fold between 5 and 150 mM KCl, the specificity and fidelity of cleavage remain constant. Thus, restrictocin maintains its cleavage specificity and fidelity over a broad range of salt and pH conditions, including those resembling physiological conditions (pH ∼7.4 and monovalent salt concentration of ∼130 mM).

SRL Recognition Occurs during Conversion of the Bound Complex into Products. Gluck et al. (*22*) have established that α-sarcin recognizes the SRL structure by binding to the bulged-G and using it for orientation. The ribotoxin then cleaves the GAGA tetraloop at a fixed distance and in a fixed position in space (*22*). We further examined the role of the SRL sequence and structure in the recognition event using the framework developed here. We disrupted the SRL incrementally and studied the effects on restrictocin binding and cleavage. As a first step, we prepared a SRL variant that contained several sequence alterations designed to disrupt the SRL fold [designated scrSRL (Figure 6A)]. The scrSRL binds to restrictocin with an unaltered affinity but reacts 1000-fold slower. This result parallels the observations with the ssRNA 27-mer described above and directly supports our previous conclusions that the SRL fold is recognized after the initial nonspecific binding step.

In a second set of experiments designed to highlight the gross features of SRL recognition by restrictocin, we started from the basal GpA dinucleotide (S1 in Figure 6B) and added SRL sequence elements incrementally. In the presence of a saturating amount of restrictocin, GpA reacts 5-fold slower than ssRNA, presumably due to the inability of GpA to contact K113 (M. J. Plantinga, A. V. Korennykh, J. A. Piccirilli, and C. C. Correll, manuscript in preparation). Addition of the tetraloop sequence to GpA (S2) restores cleavage to the level of ssRNA, apparently by restoring interaction with K113 (M. J. Plantinga, A. V. Korennykh, J. A. Piccirilli, and C. C. Correll, unpublished results). The next increment (S3) restored the bulged-G motif and the accompanying noncanonical base pairs. S3 reacts 10-fold faster than S2 and ssRNA; this enhancement disappears upon disruption of the CG base pair that closes the tetraloop (S4). Interestingly, substitution of the bulged-G motif of S3 with a Watson−Crick stem (S5) gave a 2-fold advantage over S3 and a 23-fold advantage over ssRNA. This finding suggests that the tetraloop alone can impart specificity (1.9 kcal/mol), though not as effectively as the entire SRL (4.3 kcal/mol). Addition of the Watson−Crick stem to S3 (S6) restores the full SRL, enhancing cleavage by 83-fold (2.7 kcal/mol). Further extension of the Watson−Crick stem to a total of 10 bp results in a 37-mer SRL that exhibits the same cleavage kinetics as S6 ($k_{cat} = 0.8 \pm 0.2\ s^{-1}$, $K_m = 10 \pm 3$ nM), suggesting that five Watson−Crick bases in S6 are sufficient for maximum reactivity. According to structural modeling, this Watson−Crick stem lies outside the restrictocin−SRL interface. Therefore, this element may impart specificity indirectly by stabilizing the SRL fold. The ribotoxin "recognizes" the GAGA tetraloop of the SRL by 23-fold (1.9 kcal/mol) compared to ssRNA. The bulged-G enhances the cleavage specificity by an additional 44-fold (2.4 kcal/mol). Both the GAGA tetraloop and the G-bulge are recognized during conversion of the nonspecific complex E:S into products.

Intrinsic Ribonuclease Activity of Restrictocin: Comparison to RNases T1 and U2. Restrictocin has an active site structure and composition that closely resemble those of RNases T1 and U2 (*21*). RNases T1 and U2 catalyze the cleavage of unstructured RNA after guanosine and adenosine residues, respectively. We compared the catalytic efficiencies of the ribotoxins and ribonucleases T1 and U2 during cleavage of the RNase-preferred substrate, unstructured RNA. Table 2 summarizes the catalytic constants for these enzymes. Restrictocin and α-sarcin cleave non-SRL RNA substrates 10^3−10^6-fold slower than do ribonucleases T1 and U2. Only with the SRL do the ribotoxins achieve comparable catalytic efficiency. These observations suggest that ribotoxins adapt the RNase T1-like active site to exhibit poor ribonuclease activity (Table 2), unless they encounter the elements of the SRL (Discussion).

DISCUSSION

We have characterized the kinetic pathway for cleavage of the SRL oligonucleotide catalyzed by restrictocin. At pH 7.4 and under otherwise optimal buffer and temperature conditions (37 °C and ≤5 mM KCl), the kinetics of SRL cleavage follows classic Michaelis−Menten behavior, with release of substrate (S) and products (P_1 and P_2) occurring faster than conversion of the binary E:S complex to products. P_1 and P_2 exhibit little affinity for one another, either on or off the enzyme. Under the assay conditions, they bind randomly and independently to restrictocin and with less affinity than does the SRL. Once bound, P_1 and P_2 undergo nonspecific degradation at a rate 10^3-fold slower than that of the specific cleavage of the E:SRL complex. Restrictocin also shows a modest ability to catalyze opening of the 2′,3′-cyclic phosphate at the P_1 terminus.

Formation of a Nonspecific E:S Complex (Electrostatics). We showed previously that salt has a dramatic impact on

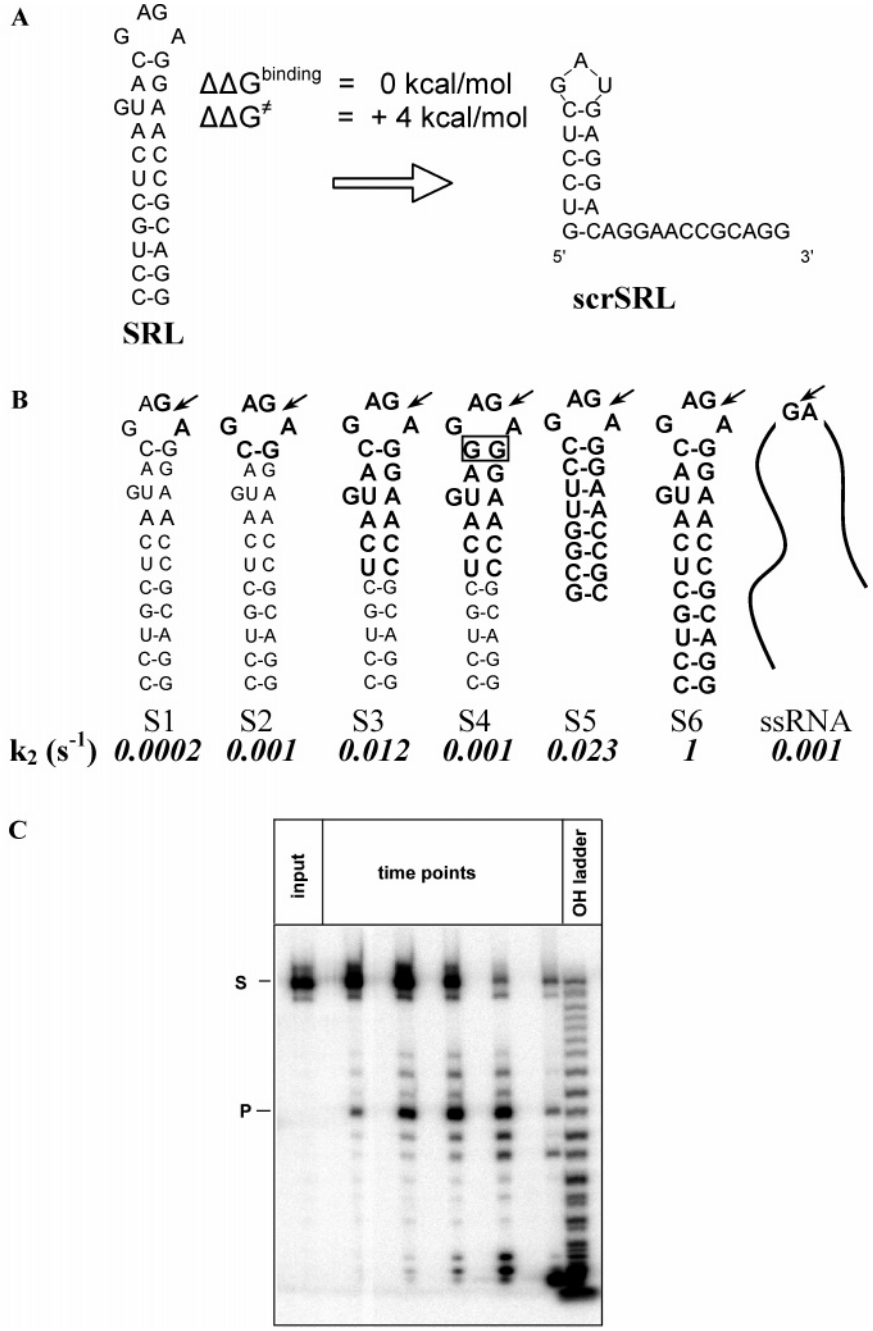

FIGURE 6: SRL sequence determinants of restrictocin specificity. (A) Binding and reactivity of a RNA derived from scrambling the SRL sequence. Scrambling the SRL sequence has no energetic consequences for restrictocin binding but eliminates SRL-derived specificity. The secondary structure of the scrambled SRL was assigned using RNAstructure 4.11. Experimental support for this assignment was obtained using a RNase T1 protection assay (not shown). (B) Reactivity of restrictocin substrates derived from incremental addition of SRL elements to the GpA basal sequence. Arrows denote the cleavage sites used to measure k_2. S1 refers to the dinucleotide pGpA. S2 contains the GAGA tetraloop and CG closing pair. S3 contains the SRL lacking the Watson−Crick stem. S4 contains the SRL lacking the Watson−Crick stem and the CG closing pair (rectangle). S5 contains the GAGA tetraloop closed by eight Watson−Crick base pairs. S6 refers to the wild-type SRL. Full substrate sequences are shown in bold. Reactions were conducted as described in the legend of Figure 3A. (C) Restrictocin retains cleavage site specificity against a RNA hairpin containing a GAGA tetraloop without the bulged-G motif (S3). S and P indicate [5′-^{32}P]S3 and the corresponding 5′-cleavage product, respectively.

the second-order rate constant of the SRL cleavage by restrictocin. Under a physiological salt concentration (∼130 mM), the SRL oligonucleotide undergoes toxin-mediated scission with a second-order rate constant of $\sim 10^2$ M^{-1} s^{-1}, but as the logarithm of the salt concentration decreases, the logarithm of the second-order rate constant increases linearly until the second-order rate constant reaches the physical limit of 10^8-10^9 M^{-1} s^{-1}. Salt affects only the binding of the toxin to the SRL RNA and not the subsequent catalytic steps. The observed dependence of log k_{obs} on log[KCl] suggests that Coulomb interactions mediate the association of the ribotoxin and the SRL RNA in the ground state complex.

The ground state complex has little specificity for SRL sequence or structure. At low salt concentrations, DNA and RNA oligonucleotides of >25 nucleotides bind to the toxin with the same affinity as the SRL even though they bear no sequence or structural resemblance to the SRL (*24*). Binding affinity and the salt dependence (n) attenuate (Figure S3) as

Table 1: RNA Oligonucleotides Used in Building the Kinetic Framework in Scheme 1

5′ → 3′	comment
^{32}P(CCUGCUCAGUACGAGAGGAACCGCAGG)	5′-labeled SRL
(CCUGCUCAGUACGAGAGGAACCGCAGG)^{32}PCo[a]	3′-labeled SRL
(CCUGCUCAGUACGAG)^{32}P(AGGAACCGCAGG)	internally labeled SRL (SRL^{p})
^{32}P(CCUGCUCAGUACGAG>P)[b]	P_1[c]
(CCUGCUCAGUACGAG)>^{32}P	P_1[d]
AGGAACCGCAGG	P_2
(AGGAACCGCAGG)^{32}PCo	P_2[e]
GUACUGAGCAGG	12-CMP
CCUGCUCAGUACGAG	5Lig
^{32}P(AGGAACCGCAGG)	3Lig
TdGdCdGdGTTdCdCTdCTdCdGTdAdCTdGdAdG	DNA splint

[a] Co represents cordycepin. [b] >P represents 2′,3′-cyclic phosphate. SRL, P_2, 12-CMP, 5Lig, and 3Lig were purchased from Dharmacon Inc. and purified by nondenaturing PAGE. DNA splint was purchased from IDT. Oligonucleotides used in restrictocin or RNaseT1 cleavage assays were radiolabeled at the 5′-end with [γ-^{32}P]ATP or at the 3′-end with [α-^{32}P]CoTP. [c] P_1 was generated by restrictocin cleavage of the 5′-radiolabeled SRL. [d] P_1 was generated by restrictocin cleavage of the internally labeled SRL constructed via ligation (Materials and Methods). [e] P_2 was generated by restrictocin cleavage of the 3′-radiolabeled SRL. 12-CMP contains sequence complementary to nucleotides 1−12 of SRL. 5Lig contains nucleotides 1−15 of SRL, 3Lig nucleotides 16−27 of SRL, and DNA splint a sequence complementary to nucleotides 5−25 of SRL.

Table 2: Comparison of the Catalytic Constants of Restrictocin with Those of α-Sarcin and Nontoxic Ribonucleases T1 and U2[a]

enzyme	substrate	k_2 or k_{cat} (s^{-1})
restrictocin[b]	pGpA	0.0002 (k_2)
restrictocin[b]	GpA within ssRNA	0.001 (k_2)
restrictocin[b]	SRL	1 (k_2)
restrictocin[b]	SRL	1.6 (k_{cat})
restrictocin[b]	80S rat liver ribosomes	1 (k_{cat})
α-sarcin[b]	SRL	0.06 (k_2)
α-sarcin[c]	pApA	0.00027 (k_2)
RNase U2[d]	ApA	0.3 (k_{cat})
RNase T1[e]	GpA	96 (k_{cat})

[a] Restrictocin recognizes the SRL during the k_2 step; accordingly, we compare catalytic constants rather than binding constants or second-order rate constants here. [b] Values were determined during our work. Reactions were conducted at 37 °C, and mixtures contained 10 mM Tris-HCl (pH 7.4) and 0.05% Triton X-100. Ribosome reaction mixtures contained in addition 50 mM KCl and 1 mM $MgCl_2$ (*24*). [c] From ref *36*. [d] From ref *37*. [e] From ref *11*.

substrate length decreases, further supporting the conclusion that Coulomb interactions between the positively charged ribotoxin surface and the negatively charged RNA stabilize the ground state complex (E:S). The lack of specificity for the SRL sequence or structure in this ground state complex does not preclude the possibility that restrictocin uses specific residues to mediate the Coulomb interactions. These features also govern binding of P_1 and P_2 to restrictocin.

Formation of a Nonspecific E:S Complex (Association and Dissociation Kinetics). Characterization of a SRL substrate containing a 3′-bridging phosphorothioate (3′S-SRL) at the cleavage site allowed us to gain insight into the kinetics that govern the formation and breakdown of the initial nonspecific complex. As the pH decreases from 7.4 to 6.7, the rate-limiting step for the reaction E + 3′S-SRL changes from the k_2 step to a step limited by diffusion. Under diffusion-limited conditions, the observed $k_2/K_{1/2}$ value of 1.1×10^9 M^{-1} s^{-1} represents the second-order rate constant for the formation of the E:S complex. This rate of association exceeds that for most binary macromolecular complexes and approaches the rate of bimolecular encounters predicted from the Smoluchowski equation (9.8×10^9 M^{-1} s^{-1}). These observations highlight the major role of electrostatics during cleavage of the SRL RNA. We estimated that the SRL dissociates from the E:S complex with a k_{off} of ~8 s^{-1}.

Electrostatics and Other Ribonucleases. In contrast to our findings for restrictocin, electrostatic forces appear to oppose binding between RNA oligonucleotides and RNase T1, a well-characterized ribonuclease used frequently for comparison to ribotoxins. We find that KCl or spermine hydrochloride enhances the second-order rate constant for RNase T1-catalyzed cleavage of 27-mer ssRNA (Figure S9). These salts may screen the repulsive interactions between the negatively charged RNase T1 (pI_{calc} 4.2) and RNA. Notably, restrictocin (pI_{calc} 9.13) also stimulates the RNase T1-catalyzed cleavage of the ssRNA 27-mer, suggesting that the cationic groups of the ribotoxin may act in a manner analogous to that of spermine and screen the repulsive interactions between RNase T1 and RNA (Figure S9C). The possibility that cleavage in Figure S9C arises from restrictocin activity is unlikely, as the ribotoxin cleaves the ssRNA at a rate much slower ($k_2 = 0.001$ s^{-1}) than the k_{obs} in the experiment. These findings show a significant functional difference between restrictocin and the nontoxic ribonuclease T1.

Ribonuclease A (*33*), barnase (*34*), and a well-studied DNA-binding protein *lac* repressor (*35*) also use electrostatic interactions for binding. Binding of these proteins to their respective targets occurs in two substeps. The first substep results in a loose electrostatically stabilized complex E:S, which serves to lower the barrier for the association (*34*). The second step involves rearrangement of E:S to give the stable ground state complex E·S (*33*−*35*). The transition from E:S to E·S presumably includes expulsion of water from the molecular interface and formation of short-range contacts between E and S (*34*). Consistent with the association mechanisms of these proteins, our results implicate the formation of a nonspecific electrostatically stabilized complex E:S. However, unlike the case in the examples described above, instead of converting to a specific ground state complex E·S, the complex E:S formed by restrictocin and SRL rearranges to the specific complex E·S only transiently, en route to the chemical transition state (restrictocin binds to SRL and nonspecific RNA with the same affinity; see Figure 6A for example). This finding could explain the difficulty in obtaining restrictocin−SRL cocrystals in which restrictocin would contact both the bulged-G and the GAGA tetraloop simultaneously. Such a complex would mimic a transient state rather than the ground state of the reaction and, therefore, would be unstable.

Energetic Contribution of SRL Structural Elements to Specific Cleavage. Specific recognition of the SRL occurs after the ground state complex forms, during the conversion of the E:S complex to products. The toxin−SRL complex reacts with a first-order rate constant (k_{cat}) of 1.6 ± 0.4 s^{-1}, approximately 10^3-fold faster than the rate of the reaction of a GA dinucleotide embedded in the context of single-stranded oligonucleotides of comparable length. Structural elements of the SRL contribute 4.3 kcal/mol to specific cleavage of the binary complex E:S. The binary complex

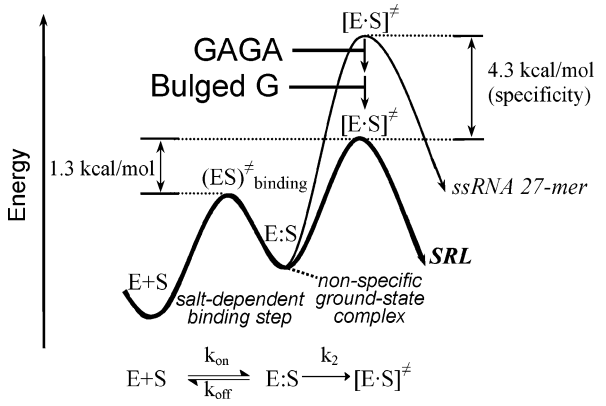

FIGURE 7: Schematic representation of the free energy diagrams for the restrictocin-catalyzed cleavage of wild-type SRL (thick line) as compared to that for a nonspecific substrate (ssRNA, thin line). To simplify comparison, the E + S states are given the same free energy. $(ES)^{\neq}$ binding represents the transition state for binding, $[E{\cdot}S]^{\neq}$ represents the transition state for cleavage. E:S represents the ground state complex stabilized by Coulomb interactions and has an identical free energy (relative to the E + S state) for oligonucleotides of the same length, including SRL and ssRNA. The free energy difference between k_2 (1 s^{-1}) and k_{off} (8 s^{-1}) is ~1.3 kcal/mol.

should undergo one or more conformational changes that would dock the SRL specifically before or during the cleavage event. Whether this or a subsequent step limits the rate of the reaction remains unknown. However, experiments with the 3′S-SRL suggest that under the standard conditions of our experiments (pH 7.4), the chemical step most likely limits the reaction rate.

We applied the developed quantitative framework to assess what elements of the SRL contribute to specificity. Wool and colleagues had previously established the importance of the bulged-G motif to specific cleavage, and our data support their conclusions. We now find that a Watson−Crick stem closed by a GAGA tetraloop also imparts specificity to restrictocin cleavage, reacting 23-fold faster than ssRNA (1.9 kcal/mol). As this substrate lacks a bulged-G motif, the results imply that the tetraloop itself may contribute energetically to SRL cleavage. Assuming that the GAGA tetraloop and bulged-G motif contribute independently to transition state stabilization, we obtain a lower limit of 2.4 kcal/mol (4.3 kcal/mol − 1.9 kcal/mol) for the contribution of the bulged-G motif to the specificity.

These observations allow us to refine further the model of recognition of SRL by the ribotoxins. The identity element (bulged-G) apparently does not serve for binding of the ribotoxin, which has been suggested by the molecular ruler model. Instead, contacts to the bulged-G form during conversion of the ground state of the reaction to the transition state, i.e., during the postbinding k_2 step, providing the specificity (Figure 7). The bulged-G is not strictly required for the cleavage site selection within the GAGA tetraloop but increases the rate and specificity of SRL cleavage.

Ribotoxins Couple Catalysis to the SRL Structure. Restrictocin and α-sarcin are strikingly inefficient ribonucleases during cleavage of RNA dinucleotides or single-stranded RNA oligonucleotides, compared to RNases T1 and U2. The SRL structure enhances catalysis at the active sites of the ribotoxins, providing an up to ~4000-fold (5.2 kcal/mol) advantage over nonspecific substrates (Table 2). Apparently, the ribotoxins acquired a mechanism for suppressing activity of their RNase T1/U2-like active sites, until the GAGA tetraloop and the bulged-G bind; i.e., they couple catalysis at their active sites to the SRL structure. Establishing the molecular basis of this functional coupling is an appealing future goal.

ACKNOWLEDGMENT

We thank Professor I. G. Wool and Dr. Yuen-Ling Chan for the gift of restrictocin and α-sarcin and members of the Piccirilli and Correll laboratory for comments on the manuscript. We thank Professors David Baker (author of APBS), Steven Kron, and Norbert Scherer for valuable discussions.

SUPPORTING INFORMATION AVAILABLE

Supplementary Figures S1−S9. This material is available free of charge via the Internet at http://pubs.acs.org.

REFERENCES

1. Sun, W., Pertzev, A., and Nicholson, A. W. (2005) Catalytic mechanism of *Escherichia coli* ribonuclease III: Kinetic and inhibitor evidence for the involvement of two magnesium ions in RNA phosphodiester hydrolysis, *Nucleic Acids Res. 33*, 807−815.
2. Zahler, N. H., Sun, L., Christian, E. L., and Harris, M. E. (2005) The pre-tRNA nucleotide base and 2′-hydroxyl at N(-1) contribute to fidelity in tRNA processing by RNase P, *J. Mol. Biol. 345*, 969−985.
3. Lee, B., Matera, A. G., Ward, D. C., and Craft, J. (1996) Association of RNase mitochondrial RNA processing enzyme with ribonuclease P in higher ordered structures in the nucleolus: A possible coordinate role in ribosome biogenesis, *Proc. Natl. Acad. Sci. U.S.A. 93*, 11471−11476.
4. Sidrauski, C., and Walter, P. (1997) The transmembrane kinase Ire1p is a site-specific endonuclease that initiates mRNA splicing in the unfolded protein response, *Cell 90*, 1031−1039.
5. Le Roy, F., Salehzada, T., Bisbal, C., Dougherty, J. P., and Peltz, S. W. (2005) A newly discovered function for RNase L in regulating translation termination, *Nat. Struct. Mol. Biol. 12*, 505−512.
6. Paushkin, S. V., Patel, M., Furia, B. S., Peltz, S. W., and Trotta, C. R. (2004) Identification of a human endonuclease complex reveals a link between tRNA splicing and pre-mRNA 3′ end formation, *Cell 117*, 311−321.
7. Acharya, K. R., Shapiro, R., Allen, S. C., Riordan, J. F., and Vallee, B. L. (1994) Crystal structure of human angiogenin reveals the structural basis for its functional divergence from ribonuclease, *Proc. Natl. Acad. Sci. U.S.A. 91*, 2915−2919.
8. Holloway, D. E., Chavali, G. B., Hares, M. C., Baker, M. D., Subbarao, G. V., Shapiro, R., and Acharya, K. R. (2004) Crystallographic studies on structural features that determine the enzymatic specificity and potency of human angiogenin: Thr44, Thr80, and residues 38−41, *Biochemistry 43*, 1230−1241.
9. Yamanishi, H., and Yonesaki, T. (2005) RNA cleavage linked with ribosomal action, *Genetics 171*, 419−425.
10. Scadden, A. D., and Smith, C. W. (1997) A ribonuclease specific for inosine-containing RNA: A potential role in antiviral defence? *EMBO J. 16*, 2140−2149.
11. Steyaert, J., Opsomer, C., Wyns, L., and Stanssens, P. (1991) Quantitative analysis of the contribution of Glu46 and Asn98 to the guanosine specificity of ribonuclease T1, *Biochemistry 30*, 494−499.
12. Raines, R. T. (1998) Ribonuclease A, *Chem. Rev. 98*, 1045−1066.
13. Pham, J. W. P., Janice, L., Lee, Y. S., Carthew, R. W., and Sontheimer, E. J. (2004) A Dicer-2-dependent 80S complex cleaves targeted mRNAs during RNAi in *Drosophila*, *Cell 117*, 83−94.
14. Wool, I. G. (1997) *Structure and Mechanism of Action of the Cytotoxic Ribonuclease* α-*Sarcin*, Academic Press, Inc., San Diego.

15. Lin, Y. L., Elias, Y., and Huang, R. H. (2005) Structural and Mutational Studies of the Catalytic Domain of Colicin E5: A tRNA-Specific Ribonuclease, *Biochemistry 44*, 10494−10500.
16. Anantharaman, V., Koonin, E. V., and Aravind, L. (2002) Comparative genomics and evolution of proteins involved in RNA metabolism, *Nucleic Acids Res. 30*, 1427−1464.
17. Klein, D. J., Schmeing, T. M., Moore, P. B., and Steitz, T. A. (2001) The Kink-Turn: A New RNA Secondary Structure Motif, *EMBO J. 20*, 4214−4221.
18. Olmo, N., Turnay, J., González De Buitrago, G., de Silanes, I. L., Gavilanes, J. G., and Lizarbe, M. A. (2001) Cytotoxic mechanism of the ribotoxin α-sarcin: Induction of cell death via apoptosis, *Eur. J. Biochem. 268*, 2113−2123.
19. Stirpe, F. (2004) Ribosome-inactivating proteins, *Toxicon 44*, 371−383.
20. Nielsen, K. B., and Boston, R. S. (2001) Ribosome-Inactivating Proteins: A Plant Perspective, *Annu. Rev. Plant Physiol. 52*, 785−816.
21. Yang, X., Gerczei, T., Glover, L., and Correll, C. C. (2001) Crystal structures of restrictocin-inhibitor complexes with implications for RNA recognition and base flipping, *Nat. Struct. Biol. 8*, 968−973.
22. Gluck, A., and Wool, I. G. (1996) Determination of the 28 S ribosomal RNA identity element (G4319) for α-sarcin and the relationship of recognition to the selection of the catalytic site, *J. Mol. Biol. 256*, 838−848.
23. Yang, X., and Moffat, K. (1996) Insights into specificity of cleavage and mechanism of cell entry from the crystal structure of the highly specific *Aspergillus* ribotoxin, restrictocin, *Structure 4*, 837−852.
24. Korennykh, A. V., Piccirilli, J. A., and Correll, C. C. (2006) The electrostatic character of the ribosomal surface enables extraordinarily rapid target location by ribotoxins, *Nat. Struct. Mol. Biol. 13*, 436−443.
25. Lukavsky, P. J., and Puglisi, J. D. (2004) Large-scale preparation and purification of polyacrylamide-free RNA oligonucleotides, *RNA 10*, 889−893.
26. Tsibul'kin, E. K., Sibileva, M. A., Vlasova, N. V., and Kozhatov, A. D. (1982) Measurements of the viscosity of erythrocyte suspensions using the Ostwald viscosimeter, *Probl. Gematol. Pereliv. Krovi 27*, 52−56.
27. Holbrook, J. A., Tsodikov, O. V., Saecker, R. M., and Record, M. T., Jr. (2001) Specific and non-specific interactions of integration host factor with DNA: Thermodynamic evidence for disruption of multiple IHF surface salt-bridges coupled to DNA binding, *J. Mol. Biol. 310*, 379−401.
28. Endo, Y., Huber, P. W., and Wool, I. G. (1983) The ribonuclease activity of the cytotoxin α-sarcin. The characteristics of the enzymatic activity of α-sarcin with ribosomes and ribonucleic acids as substrates, *J. Biol. Chem. 258*, 2662−2667.
29. Lacadena, J., Martinez del Pozo, A., Lacadena, V., Martinez-Ruiz, A., Mancheno, J. M., Onaderra, M., and Gavilanes, J. G. (1998) The cytotoxin α-sarcin behaves as a cyclizing ribonuclease, *FEBS Lett. 424*, 46−48.
30. Weinstein, L. B., Earnshaw, D. J., Cosstick, R., and Cech, T. R. (1996) Synthesis and Characterization of an RNA Dinucleotide Containing a 3′-S-Phosphorothiolate Linkage, *J. Am. Chem. Soc. 118* (43), 10341−10350.
31. Steyaert, J., Wyns, L., and Stanssens, P. (1991) Subsite interactions of ribonuclease T1: Viscosity effects indicate that the rate-limiting step of GpN transesterification depends on the nature of N, *Biochemistry 30*, 8661−8665.
32. Miller, S. P., and Bodley, J. W. (1988) α-Sarcin cleaves ribosomal RNA at the α-sarcin site in the absence of ribosomal proteins, *Biochem. Biophys. Res. Commun. 154*, 404−410.
33. Park, C., and Raines, R. T. (2003) Catalysis by ribonuclease A is limited by the rate of substrate association, *Biochemistry 42*, 3509−3518.
34. Selzer, T., and Schreiber, G. (1999) Predicting the rate enhancement of protein complex formation from the electrostatic energy of interaction, *J. Mol. Biol. 287*, 409−419.
35. von Hippel, P. H. (2004) Biochemistry. Completing the view of transcriptional regulation, *Science 305*, 350−352.
36. Masip, M., Garcia-Ortega, L., Olmo, N., Garcia-Mayoral, M. F., Perez-Canadillas, J. M., Bruix, M., Onaderra, M., Martinez del Pozo, A., and Gavilanes, J. G. (2003) Leucine 145 of the ribotoxin α-sarcin plays a key role for determining the specificity of the ribosome-inactivating activity of the protein, *Protein Sci. 12*, 161−169.
37. Yasuda, T., and Inoue, Y. (1982) Studies of catalysis by ribonuclease U2. Steady-state kinetics for transphosphorylation of oligonucleotide and synthetic substrates, *Biochemistry 21*, 364−369.

BI700931Y